Supporting Information

Microflower-like Co_9S_8@MoS_2 heterostructure as an efficient bifunctional catalyst for overall water splitting

Chaohai Pang,‡ [a,b*] Xionghui Ma,‡ [a,b] Yuwei Wu, [a,b] Shuhuai Li, [a,b*] Zhi Xu, [a,b] · Mingyue Wang, [a,b] · Xiaojing Zhu,[c*]

[a] *Analysis and Test Center, Chinese Academy of Tropical Agricultural Sciences, Hainan Provincial Key Laboratory of Quality and Safety for Tropical Fruits and Vegetables, Key Laboratory of Quality and Safety Control for Subtropical Fruit and Vegetable,Ministry of Agriculture and Rural Affairs Haikou, 571101, China*

[b] *Key Laboratory of Tropical Fruits and Vegetables Quality and Safety for State Market Regulation, Haikou, 570311, China*

[c] *Research Center of Advanced Chemical Equipment, Chemistry and Chemical Engineering Guangdong Laboratory, Shantou 515041, China*

Address correspondence to E-mail: 18389859589@163.com; happylishuhuai@163.com; xiaoj_zhu@163.com

‡ C.P and X.M contributed equally to this work.

Experimental section

Materials

Cobalt nitrate hexahydrate (Co $(NO_3)_2 \cdot 6H_2O$, 99%) and ethanol were obtained from Aladdin Chemical Co. Sodium molybdate dihydrate ($Na_2MoO_4 \cdot 2H_2O$, 99.5%), formaldehyde (36%–38%), thiourea (99%), and ethylenediamine (99%) were obtained from Sigma-Aldrich Chemical Co. The commercial Pt/C powder (20wt%) was provided by Shanghai Macklin Biochemical Technology Co., Ltd.

Preparation of $Co_9S_8@MoS_2$

In a typical experiment, Co $(NO_3)_2 \cdot 6H_2O$, thiourea, and $Na_2MoO_4 \cdot 2H_2O$ were added to 40 mL of deionised water, and the mixture was thoroughly stirred for even dispersion. Subsequently, ethylenediamine and formaldehyde were added dropwise under continuous stirring. The final molar ratio of thiourea/Co/ethylenediamine/formaldehyde/Mo was 1.5:1:1:2:0.001. Subsequently, the mixture was poured into a stainless steel autoclave (50 mL) lined with polytetrafluoroethylene and then reacted at 180 °C for one day. The obtained sample was washed with deionised water and ethanol and then desiccated in an oven. Finally, the $Co_9S_8@MoS_2$ heterostructure was pyrolyzed at 2 °C min^{-1} to 500 °C and held for 2 h in nitrogen atmosphere.

Corresponding Co_9S_8 and MoS_2 materials were fabricated using the same procedure, but lacking $Na_2MoO_4 \cdot 2H_2O$ and Co $(NO_3)_2 \cdot 6H_2O$, respectively. And the synthesized processes of $Co_9S_8@MoS_2$-low and $Co_9S_8@MoS_2$-high were similar to those of $Co_9S_8@MoS_2$ heterostructure while the final molar ratio was correspondingly changed to1.5:1:1:2:0.0005 and 1.5:1:1:2:0.0015.

Material characterisation

To characterise the crystal structures of the composites, X-ray diffraction (XRD) was recorded on a Rigaku RINT 2000 instrument (Cu Kα radiation, 40 kV, 40 mA). The microstructures of $Co_9S_8@MoS_2$ were investigated using Hitachi SU-8000 electron microscopy. Elemental mapping and transmission electron microscopy (TEM) were

carried out using a JEM-2100F microscope operated at 200 kV. The composition of Co_9S_8@MoS_2 was evaluated using X-ray photoelectron spectroscopy (XPS; Phi X-tool). The surface areas and pore size distribution were determined by the Brunauer-Emmett-Teller (BET) and Barrett-Joyner-Halenda (BJH) method, respectively, using N_2 isotherm measured with a Micromeritics ASAP 2460 analyser (USA).

Electrochemical measurements

In a three-electrode system, the HER and OER activities of Co_9S_8@MoS_2 were investigated on a CHI 750E electrochemical workstation at ambient temperature. To prepare the electrocatalyst ink, 4 mg of the composite material was suspended in 1.0 mL of 0.05 wt.% Nafion in ethanol by ultrasonication. Then, the catalyst ink was drop-cast onto a glassy carbon electrode (GCE) and dried at 30 °C to obtain a catalyst loading of 404 μg cm^{-2}. In alkaline medium, the modified GCE was used as the working electrode, an Ag/AgCl electrode as the reference electrode and a graphite rod as the counter electrode. When the electrocatalytic measurements were conducted under acidic conditions, a saturated calomel electrode was utilised as the counter electrode instead of the graphite rod. The potentials measured in 1 M KOH and 0.5 M H_2SO_4 were converted to the reversible hydrogen electrode (RHE) scale based on the equations: $E_{RHE} = E_{Ag/AgCl} + 0.1976 + 0.059 \times pH$ and $E_{RHE} = E_{SCE} + 0.241 + 0.059 \times pH$. All potentials were recorded at a scan rate of 10 mV s^{-1}.

The electrochemical double-layer capacitance (C_{dl}) of each sample was tested by employing cyclic voltammetry at non-Faradaic potentials between 0.3 and 0.5 V at sweep rates from 20 to 100 mV s^{-1}. The discrepancy in current density between the cathodic and anodic sweeps at 0.35 V vs. RHE in 1 M KOH was plotted against the scan rate, and the slope of the linear regression line was obtained. The value of the slope is twice that of C_{dl}.

In a two-electrode system, the overall water splitting measurements were organised in 1.0 M KOH. A nickel foam (0.4 cm^2) loaded with 0.4 mg of electrocatalyst was utilised as the working electrode.

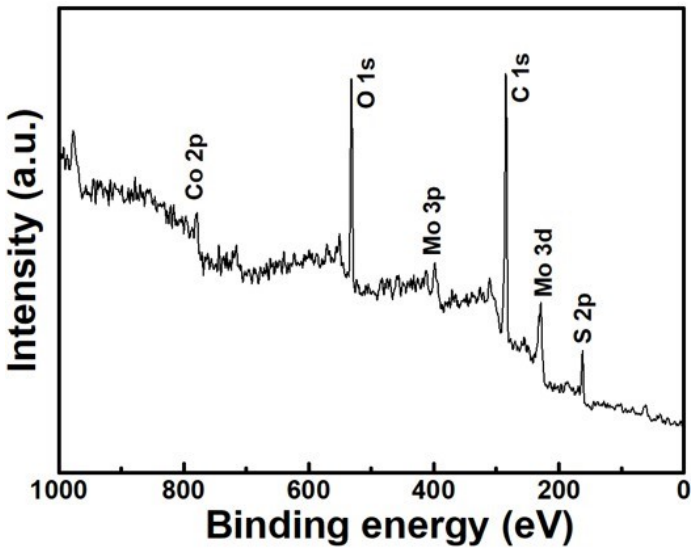

Figure S1. XPS spectrum of the obtained Co_9S_8@MoS_2 heterostructure.

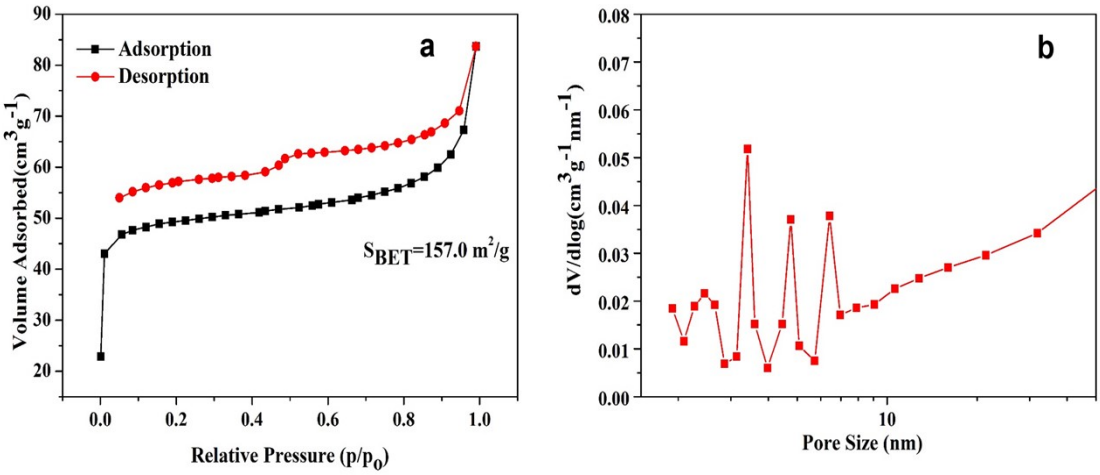

Figure S2. (a) N_2 adsorption-desorption isotherms and (b) the corresponding pore size distribution of the typical sample Co_9S_8@MoS_2.

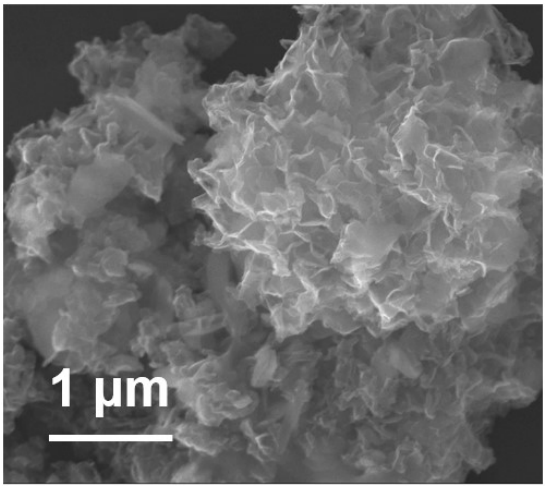

Figure S3. SEM images of Co_9S_8@MoS_2-after the catalytic OER test.

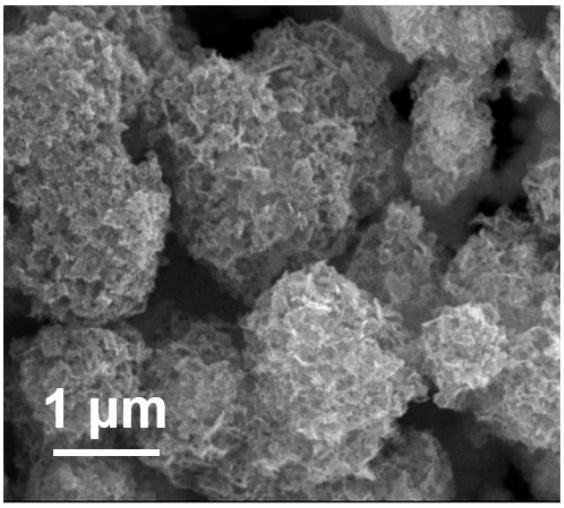

Figure S4. SEM images of Co_9S_8@MoS_2-after the catalytic HER test.

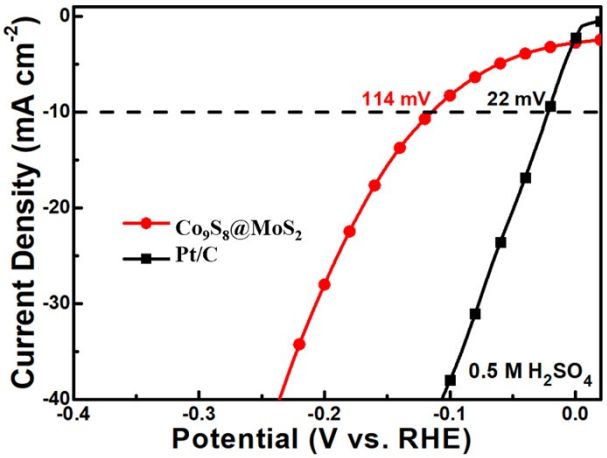

Figure S5. HER performance of Co_9S_8@MoS_2 in 0.5 M H_2SO_4.

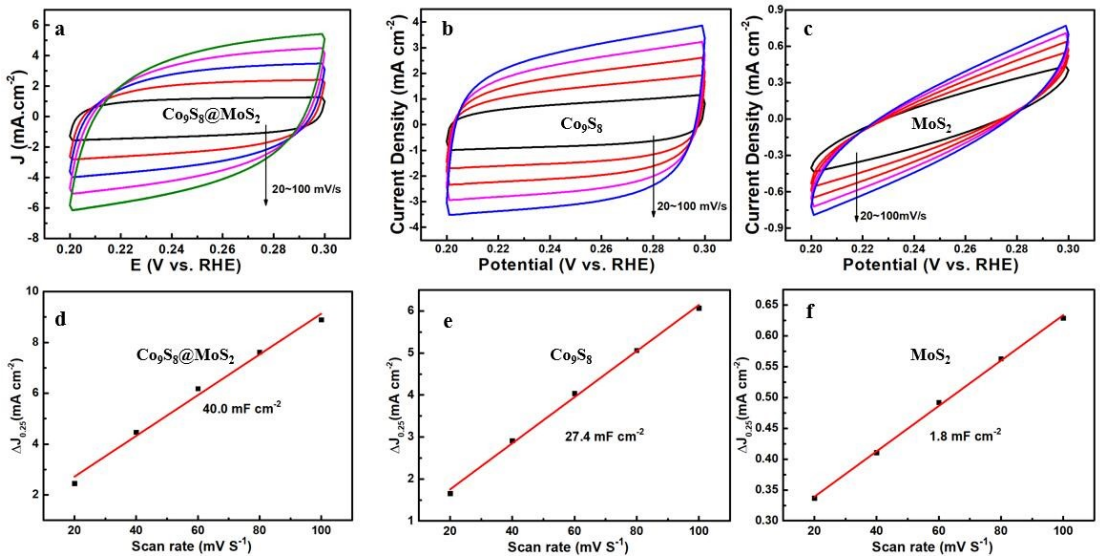

Figure S6. Cyclic voltammograms of (a) Co_9S_8@MoS_2, (b) Co_9S_8, (c) MoS_2 at different scan rates from 20 to 100 mV s^{-1}. Linear slopes were plotted from the cyclic voltammograms of (d) Co_9S_8@MoS_2, (e) Co_9S_8 and (f) MoS_2 in 1M KOH. The linear slopes are equivalent to twice the double-layer capacitance (C_{dl}).

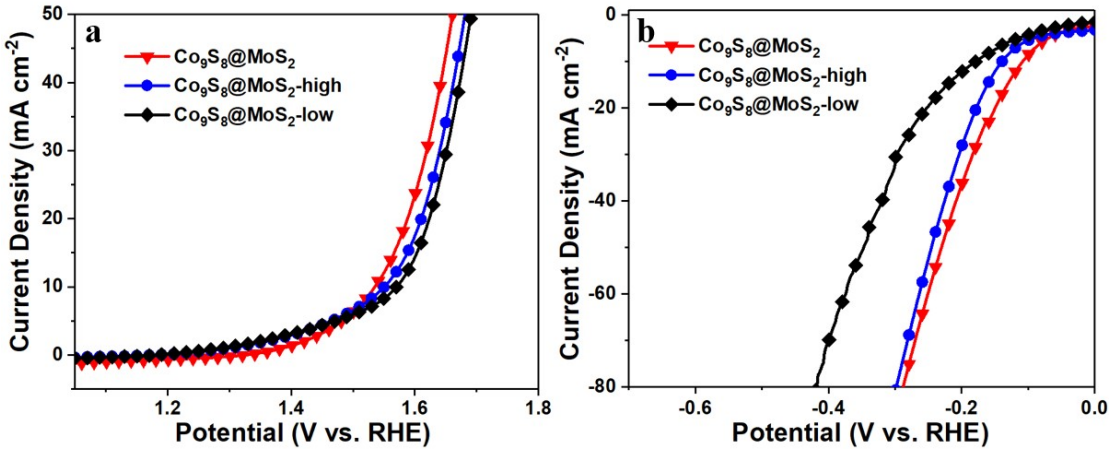

Figure S7. LSV curves of Co_9S_8@MoS_2, Co_9S_8@MoS_2-high and Co_9S_8@MoS_2-low electrodes in 1 M KOH for OER (a) and HER (b).

Table S1. The reported HER and OER of some cobalt- and molybdenum-based sulfides electrocatalysts compared with that of this study.

Catalyst	Reaction	Current density j=10 mA cm^{-2}	ŋ at corresponding j (mV)		Tafel slope ($mV \cdot dec^{-1}$)		Reference
			1M KOH	0.5M H_2SO_4	1M KOH	0.5M H_2SO_4	
Co_9S_8-MoS_2	**HER**	**10**	**103**	**114**	**124**	**127**	**This work**
	OER	**10**	**295**	**-**	**175**	**-**	
Co_9S_8-MoS_2@3DC	HER	10	177	230	83.6	111.7	1
	OER	-	-	-	-	-	
MoO_2@MoS_2@Co_9S_8	HER	10	160	-	80	-	2
	OER	10	310	-	70	-	
Co_3S_4@MoS_2	HER	10	136	-	74	-	3
	OER	10	280	-	43	-	
NiFe-LDH/$FeCoS_2$/CFC	HER	10	308	-	157	-	4
	OER	10	190	-	56	-	
Co_9S_8-Ni_3S_2-HNT_s/Ni	HER	10	85	-	83.1	-	5
	OER	50	281	-	53.3	-	
Co_9S_8@MoS_2/CNFs	HER	10	-	190	-	110	6
	OER	10	430	-	61	-	
CoSx-Ni_3S_2/NF	HER	10	204	-	133	-	7
	OER	20	280	-	105	-	
$CoMoS_4$-Ni_3S_2/NF	HER	10	158	93	169	-	8
	OER	10	200	-	63	-	
Co_9S_8@MoS_2/N	HER	10	126	-	74.1	-	9
	OER	10	233	-	56.3	-	
Co_9S_8@MoS_2	HER	10	143	171	117	123	10
	OER	10	342	-	94	-	

References

1 L. Diao, B. Zhang, Q. Sun, N. Wang, N. Zhao, C. Shi, E. Liu and C. He, *Nanoscale*, 2019, **11**, 21479-21486.

2 Y. Li, C. Wang, M. Cui, J. Xiong, L. Mi and S. Chen, *Appl. Surf. Sci*, 2020, **543**, 148804.

3 Y. Guo, J. Tang, Z. Wang, Y. Kang, Y. Bando and Y. Yamauchi, *Nano. Energy*, 2018, **47**, 494-502.

4 Z. Zhang, J. Zhou, H. Wei, Y. Dai, S. Li, H. Shi and G. Xu, *J. Mater. Sci*, 2020, **55**, 1-16.

5 J. Li, P. Xu, R. Zhou, R. Li, L. Qiu, S. Jiang and D. Yuan, *Electrochim. Acta*, 2019, **299**, 152-162.

6 H. Zhu, J. Zhang, R. Yan Zhang, M. Du, Q. Wang, G. Gao, J. Wu, G. Wu, M. Zhang, B. Liu, J. Yao and X. Zhang, *Adv. Mater*, 2015, **27**, 4752-4759.

7 S. Shit, S. Chhetri, W. Jang, N. C. Murmu, H. Koo, P. Samanta and T. Kuila, *ACS. Appl. Mater. Interfaces*, 2018, **10**, 27712-27722.

8 P. Hu, Z. Jia, H. Che, W. Zhou, N. Liu, F. Li and J. Wang, *J. Power. Sources*, 2019, **416**, 95-103.

9 M. Kim, H. Seok, C. S. Selvam, J. Cho, G. H. Choi, M. G. Nam, S. Kang, T. Kim and P. J. Yoo, *J. Power. Sources*, 2021, **493**, 229688.

10 J. Bai, T. Meng, D. Guo, S. Wang, B. Mao and M. Cao, *ACS. Appl. Mater. Interfaces*, 2018, **10**, 1678-1689.